

Gas Chromatography Simulator for Educational Purposes

Felix Ivander

Supervised by Prof. David Stone

CHM395 – Research Project in Chemistry

Department of Chemistry

University of Toronto

Acknowledgements.

I would like to thank my supervisor Prof. David Stone for his guidance that made this work possible.

Abstract.

A gas chromatography simulation tool was built for pedagogical purposes. Retention times are modelled using a linear solvation energy relationship and peak widths using Golay's plate theory equation. Modifiable variables include inlet pressure, temperature, column dimension, and carrier gas for the isothermal and temperature programmed elution, while ramp rate is exclusive for the latter. Analytes are selected from a library of about 90 compounds, and columns from about 10. The routine for further addition has also been described. The level of accuracy of the predictions is about 15% standard deviation for retention times, and 35% for peak widths, as compared to literature data. Finally, a set of supplementary virtual exercises was designed.

Table of Contents

<i>Cover Page</i>	1
<i>Acknowledgements</i>	2
<i>Abstract</i>	3
<i>Glossary</i>	5
<i>Introduction</i>	7
<i>Theory</i>	7
<i>The algorithm</i>	13
<i>Discussion</i>	15
<i>Future Work</i>	21
<i>Conclusion</i>	22
<i>References</i>	22
<i>Supplementary exercises</i>	24

Glossary.

α	Molar entropy of solution divided by universal gas constant.
a	LSER column descriptor for the hydrogen-bond accepting ability.
A	Eddy diffusion coefficient.
A	LSER solute descriptor for the hydrogen-bond accepting ability.
β	Phase ratio.
b	LSER column descriptor for the hydrogen-bond donating ability.
B	Longitudinal band broadening coefficient.
B	LSER solute descriptor for the hydrogen-bond donating ability.
c	LSER column descriptor for the intercept.
C	Mass transfer broadening coefficient.
C_S	Independent contribution of stationary phase to C .
C_M	Independent contribution of mobile phase to C .
C	LSER solute descriptor for the intercept.
d_c	Column inner diameter.
d_f	Thickness of the liquid film.
D_S	Diffusion coefficient in the stationary phase.
D_M	Diffusion coefficient in the mobile phase.
e	LSER column descriptor for polarizability.
E	See Eq. 5 .
f_v	Volumetric flow velocity.
ΔH	Molar enthalpy of solution.
H	Plate height or height equivalent to a theoretical plate.
k	Retention factor or capacity factor.
K	Equilibrium constant or partition coefficient.
l	LSER solute descriptor for cavity forming.
L_{16}	Equilibrium constant of solute on a standardized n -hexadecane stationary phase.

L	Column length.
η	Viscosity.
P	Pressure.
r	Temperature ramp rate.
R	Universal gas constant.
R'	The ratio as described in Eq. 2 .
σ	Standard deviation.
s	LSER column descriptor for permanent dipole.
S	LSER solute descriptor for permanent dipole.
t	Time.
t_M	Column dead time or column void time or hold-up time or solvent front.
t_R	Retention time.
T_R	Retention temperature. i.e. the temperature at which the analyte exits the column.
T	Temperature
T_0	Starting temperature.
v	Linear velocity.
x	Longitudinal position.

Introduction.

The significance of chromatography, the set of analytical techniques established on the separation of a mixture, cannot be overstated: HPLC to enhance and investigate product purity is routinely used in pharmaceutical industries, as are TLC and GC for drug analysis in medical and legal uses (1,2), while coupled chromatographs (e.g. HPLC-MS, GC-MS) are used in the food industry to detect adulteration (3). There are more than a dozen versions of chromatographic techniques, usually classified by the nature of the mobile phase (e.g. liquid, gaseous, supercritical), stationary phase (e.g. liquid, paper), or separation mechanism (e.g. chirality, ionic charge, size), that have been discussed at length in the literature (4,5). The subject of interest in this work is gas chromatography, that is based on the separation of a volatilized mixture in an inert carrier gas to a liquid stationary phase.

Many challenges in teaching gas chromatography remain to be addressed, which is a serious issue considering the prevalence of the technique. Subtle, but various concepts become impractical to reinforce in an experiential setting once it is noticed that a single elution can easily reach fifteen minutes. Furthermore, changing experimental conditions each run as pedagogical demonstrations may demand can either cost another fifteen minutes to have the replaced column cool, or auxiliary expenditures by cooling with liquid nitrogen. Neither are tolerable in the context of an undergraduate course (6), and therefore in this work a solution is suggested in the form of a pedagogical simulation tool that can be accessed free of charge via a web browser.

It should be noted that this has been implemented successfully by both Reijnga (7), and Yuan (8), who wrote theirs in SERAPHIM and Fortran, respectively. However, neither updated the tool since their publication 30 and 43 years ago, and thus it is unfeasible to have them run on current devices. More recent alternatives either suffered the same fate (38) or lack flexibility (39). There are also simulation packages intended for optimization purposes in research, such as Comsol (9) and DryLab (10), although their use as pedagogical tools will likely be sub-optimal since the learning curves are steep in addition to burdening the students with ancillary costs. Indeed, an effective pedagogical device should be easily accessible and simple to use.

For this reason, a GC simulator geared for pedagogical purposes was developed, and a set of virtual gas chromatography exercises, whose importance has been emphasized by Stone (6), as supplement was designed. The theoretical bases are adopted from a linear solvation energy relationship model by Abraham (11), plate theory of chromatography by Martin and Synge (17), Golay's plate theory equation (16), a temperature gradient model by Curvers and Rijks (30,31), the Hagen-Poiseuille equation (26), and some works that follow from them.

Theory

The differing sorption and desorption rates of analytes on a stationary phase underlie separation in gas chromatography. Assuming an analyte traverses the column with length L only when it is in the mobile phase with velocity equal to the linear carrier velocity v , it can be inferred that the average amount of time, t_R , an analyte spends in the column is

$$\frac{L}{v \times R'} \text{ (Eq. 1)}$$

Where R' is defined as

$$\frac{\text{av. time spent in mobile phase}}{\text{av. time spent in mobile phase} + \text{av. time spent in stationary phase}} = \frac{n(\text{mobile})}{n(\text{mobile}) + n(\text{stationary})} \quad (\text{Eq. 2})$$

For the limit $n \rightarrow \infty$. Clearly, a hypothetical unretained analyte of R' equal one traverses the column non-instantaneously. Define this duration as t_M or column dead-time. Direct determination of R' is arduous, hence to model t_R let an arbitrary physicochemical parameter k , retention factor, be defined:

$$k = \frac{t_R - t_M}{t_M} = \frac{\frac{L}{R'v} - \frac{L}{v}}{\frac{L}{v}} = \frac{n(\text{stationary})}{n(\text{mobile}) + n(\text{stationary})} \quad (\text{Eq. 3})$$

Notice that this parameter depends on the affinity of the analyte to the stationary phase but not to the mobile phase, as one would expect if the carrier gases are inert. Subsequently, k can be derived from solvation models. In this work, a linear solvation energy relationship (LSER) as proposed by Abraham (11) is used:

$$\log(SP) = c + eE + sS + aA + bB + lL_{16} \quad (\text{Eq. 4})$$

Here SP is a free-energy property of the analyte and the system. For the purposes of this work, it shall be defined as k . The variables c , e , s , a , and l all refer to properties of the stationary phase that affect solute-system interactions: c is the intercept and considers particular conditions; e considers the polarizability of the system which facilitates the potential dispersion interactions with analytes, s permanent dipole, a hydrogen-bond accepting ability, b hydrogen bond donor ability, and l is associated with cavity forming (12).

The variables E , S , A , B , and L_{16} are associated with the analytes. S considers the permanent dipole of the analyte, A the hydrogen-bond donating ability, and B the hydrogen-bond accepting ability. L_{16} is defined as the equilibrium constant of analyte-system on standardized n -hexadecane stationary phase at 298.2 K. For some analytes, mostly those that are non-volatile, experimental determination is difficult, but otherwise, it is simply capacity factor multiplied by phase ratio. E , the excess molar refraction, is defined as the molar refraction of the analyte subtracted by the molar refraction of a hypothetical n -alkane. It considers the potential van-der-Waals interactions resulting from the polarizability of the analyte. This parameter is most straightforward to compute (12):

$$E = 10L_{16} \left[\frac{n^2 - 1}{n^2 + 2} \right] - 2.832L_{16} + 0.526 \quad (\text{Eq. 5})$$

Where n is the refractive index of said analyte at 20°C for the sodium 588.9950 and 589.5924 nm lines.

As one might expect, these parameters vary with temperature. For example, van-der-Waals interactions are greatly diminished as temperature increases since molecules rotate more rapidly. In fact, it is always the case that s , a , b , and l values decrease as temperature increases (12).

Allowing these parameters to be functions of temperature then allows for k therefore t_R to be a function of temperature in isothermal elution. Data collected by Poole (34) are collected in this manner although temperature spanned only 60-140°C. Subsequently the values as predicted by this simulator are most reliable in that range.

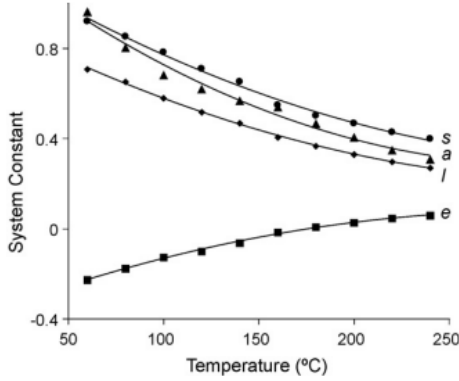


Fig. 1. System map of DB-1701 stationary phase LSER parameter values under different temperatures (12).

Indeed, one could very well define SP as the more popular partition coefficient K :

$$K = \frac{n(\text{stationary})}{n(\text{mobile})} \times \frac{V_{\text{mobile}}}{V_{\text{stationary}}} \quad (\text{Eq. 6})$$

In that case, c would be expected to differ to if SP were k . However, this would reduce the generality of the constants, as then they are valid only in certain column dimensions. Instead, K will be used to model elution done in temperature gradient.

For a temperature-programmed elution, Curvers and Rijks (13) have shown that for a single ramp, **Eq.7** holds:

$$\int_{T_0}^{T_R} \frac{dT}{t_M(T) \left[1 + \frac{\alpha}{\beta} e^{\frac{\Delta H}{RT}} \right]} = r \quad (\text{Eq. 7})$$

Where ΔH is the molar enthalpy of solution (expressed strictly positive, also denoted as enthalpy of partition), R is the universal gas constant, α is the term $\frac{\Delta S}{R}$ where ΔS is the molar entropy of solution, β is the phase ratio $\frac{V_M}{V_S}$, T_0 is the starting temperature, r is the ramp rate, T_R is the retention temperature and is described by:

$$T_R = T_0 + r \times t_R \quad (\text{Eq. 8})$$

While generally

$$T(t) = T_0 + r \times t \quad (\text{Eq. 8.5})$$

Hence, for a single-ramp temperature-programmed elution, the retention time of an analyte can be found with **Eq.7** and **Eq.8**. T_R can approximated using Simpson's rule applied on **Eq. 7**, to be discussed in greater depth in the algorithm section of the introduction. The theoretical

underpinnings of **Eq. 7**, have also been discussed by Curvers and Rijks (13) in much greater detail, and to follow is a brief overview:

Notice that **Eq. 2** can be combined with **Eq. 6** to yield the relation:

$$R = \left(\frac{K}{\beta} + 1 \right)^{-1} \quad (\mathbf{Eq. 9})$$

As a result, **Eq. 1** can be expressed as:

$$t_R = \frac{L}{v} \left(\frac{K}{\beta} + 1 \right) \quad (\mathbf{Eq. 10})$$

Which in differential form is:

$$dt = \frac{dx}{v} \left(\frac{K}{\beta} + 1 \right) \quad (\mathbf{Eq. 11})$$

The van't Hoff equation in conjunction to the Gibbs free energy equation:

$$\Delta G = -RT \ln(K) = \Delta H - T\Delta S \quad (\mathbf{Eq. 11. 5})$$

Allows for the substitution of K to **Eq. 11** such that

$$dt = \frac{dx}{v} \left(\frac{\alpha}{\beta} e^{\frac{\Delta H}{RT}} + 1 \right) \quad (\mathbf{Eq. 12})$$

Differentiating **Eq. 8.5**, and substituting to **Eq. 12** gives

$$\frac{dT}{r} = \frac{dx}{v} \left(\frac{\alpha}{\beta} e^{\frac{\Delta H}{RT}} + 1 \right) \quad (\mathbf{Eq. 13})$$

Which can be rearranged to give

$$\frac{dT}{\left(\frac{\alpha}{\beta} e^{\frac{\Delta H}{RT}} + 1 \right)} = r * \frac{dx}{v} \quad (\mathbf{Eq. 14})$$

And integrated to give

$$\int_{T_0}^{T_R} \frac{dT}{\left(\frac{\alpha}{\beta} e^{\frac{\Delta H}{RT}} + 1 \right)} = \int_0^L r * \frac{dx}{v} \quad (\mathbf{Eq. 15})$$

As the right side integrates to $r \times t_M$, the final equation **Eq. 7** results. It is noteworthy that Curvers and Rijks dismissed the approach by Grant (14), who assumed that the effect of deadtime to analyte elution is negligible and the deadtime constant, such that numerical integration of **Eq. 7** is simplified. To their credit, the first assumption is implausible for analytes that elute quickly, and the second due to the dependence of deadtime on temperature as described by the modified Poiseuille's equation assuming fluid flow in the capillary is laminar:

$$f_v = \frac{\pi}{8\eta_i(T)L\left(\frac{d_c}{2}\right)^4}(\Delta P) \text{ (Eq. 16)}$$

Where η is the viscosity of gas i and is of the form $C_{1,i} + C_{2,i}T$ (in this work, the constants are adopted from Ettre (33)), d_c is column diameter, ΔP the difference between inlet (P_0) and outlet pressure (P_1), and f_v is the volumetric flow rate that readily converts to v by division of column cross section area. In this work, deadtime is approximated by setting the temperature in **Eq.23**, equivalent to **Eq.16**, as the starting temperature.

From an experimental point of view, infinitely narrow peaks (i.e. impulse) are never seen. The literature (15) have thoroughly discussed that stochastic processes governing retention are responsible. Indeed, the Gaussian profile of the peaks is the direct implication assuming the column does not overload, which is to be kept for the successive parts of this work. There is therefore merit in briefly discussing those processes, as the broadness of the peaks is crucial to the chromatogram being discernible. Even more emphasis is put when the eluted mixture consists of closely eluting analytes, such as petrol.

One of the earliest accounts of a theoretical treatment on chromatographic band broadening was the paper by J.N. Wilson (16), which introduced non-equilibrium and longitudinal diffusion but was considered inadequate for quantitation by Giddings. To follow a year after was the Nobel-winning plate theory of chromatography by Martin and Synge (17). Despite its prevalence, the theory was considered by many to be useful only in a pedagogical context (15), as the underlying assumptions are unrealistic. The column consisting of discrete plates, is clearly invalid. The assumption that equilibrium is achieved in every plate, is also invalid, as a simple thought experiment would show that if that is indeed the case, then the profile of the chromatogram should simply be that of a constant function. Finally, plate theory accounts only for unidirectional flow, which is incomplete as longitudinal diffusion is isotropic.

Regardless, successful works that follow uphold the language of plate theory. The parameter H , plate height, has been used to describe a parameter of the gaussian profile of the peak σ , standard deviation, in the form of

$$\sigma = t_R \sqrt{\frac{H}{L}} \text{ (Eq. 17)}$$

Such that a complete description of the zone as an ideal gaussian:

$$G(t) = \frac{1}{\sqrt{(2\pi\sigma^2)}} e^{-\frac{(t-t_R)^2}{2\sigma^2}} \text{ (Eq. 18)}$$

is possible.

In this treatment, the theoretical meaning of H is of minor interest as it can be obtained experimentally by analysing the chromatogram. Indeed, this is precisely what had been done: van

Deemter et al. (18) derived from a large pool of data that H is generally a function of linear flow rate in the following form:

$$H = A + \frac{B}{v} + Cv \quad (\text{Eq. 19})$$

Where A , B , C are in-system parameters, respectively: Eddy diffusion coefficient, longitudinal band broadening coefficient, and mass transfer broadening coefficient. Eddy diffusion correlates with the multiple pathlengths an analyte can take to exit the column. Since the columns of interest in this work are open-capillary, A is assumed negligible as analyte-column interactions at reasonable injections are more adsorptive, instead of absorptive, in nature. Hence the equation developed by Golay (19) is more befitting:

$$H = \frac{B}{v} + (C_S + C_M)v \quad (\text{Eq. 20})$$

Where C_S and C_M are the independent contributions from the stationary and mobile phase to C , respectively. Golay then expanded the coefficients, by integration of mass balance equation for linear chromatography:

$$H = \frac{2D_M}{v} + \frac{2kd_f^2v}{3(1+k)^2D_S} + \frac{(1+6k+11k^2)d_c^2v}{96(1+k)^2D_M} \quad (\text{Eq. 21})$$

Where D_M is the diffusion coefficient in the mobile phase, D_S is the diffusion coefficient the stationary phase, and d_f is the thickness of the liquid film. In this work, the second term is chosen to be neglected again by positing the adsorptive nature of the analyte-stationary phase interactions, as then $d_f \rightarrow 0$. D_M can instead be computed using the Fuller-Schettler, and Giddings correlation (20,21):

$$D_M = \frac{0.00125T^{1.75} \left(\frac{1}{MW_{analyte}} + \frac{1}{MW_{carrier}} \right)^{\frac{1}{2}}}{P[(\sum V_{analytes})^{\frac{1}{3}} + (\sum V_{carrier})^{\frac{1}{3}}]} \quad (\text{Eq. 22})$$

Where $\sum V_i$ can be calculated readily by summation of atomic diffusion contributions that make up i (22). This correlation, empirically derived by Fuller-Schettler and Giddings by least-fit squares analysis from over 300 datasets, is in competition with at least those developed by Arnold (23), Gilliland (24), and Hirschfelder (25), as D_M is widely used in the physical sciences. In this work it is chosen by virtue of its accuracy in spite of computational simplicity.

Therefore, chromatographic implications of carrier gases have been implicitly considered, although not in an exhaustive manner. The final theoretical consideration to be discussed is a more robust approximation of linear flow velocity, v , that follows from Poiseuille's Law (26) as presented by Cramers (27):

$$v = \frac{3P_0 \left(\left(\frac{P_1}{P_0} \right)^2 - 1 \right)^2}{4\eta_i L \left(\left(\frac{P_1}{P_0} \right)^3 - 1 \right)} \left(\frac{d_c^2}{32} \right) \quad (\text{Eq. 23})$$

Clearly, linear velocity is a function of position in the column, as is pressure. The prediction of linear velocity by Colmsjo (30) takes that into consideration in a finite element method, although for the purposes of this work such an approach is not only unnecessary but will significantly increase computational load. It should be assumed that the main target of audience, undergraduate students, are in possession of personal computers with the barest minimum computing power. For the remainder of this paper therefore, v should be taken as *mean* linear velocity.

The algorithm.

The gas chromatography simulator was written in HTML, Javascript, and CSS. It can be accessed free of charge via this [link](#). Physicochemical constants and parameters are stored in the format of a JSON file. Those pertaining to the analytes: E, S, A, B, and L₁₆ are obtained from the data by Poole (35), Siriviboon and co-workers (36), and Vitha (12). $\sum V_{analytes}$ are calculated ahead from the tabulations by Karaiskakis (22), and boiling points and molecular weights are obtained from PubChem (37). Those pertaining to the column: c , e , s , a , and l vary linearly with temperature, so they are in the form $C_1 + C_2T$ and are adopted from the data by Poole (34). The same source is also responsible for providing the column dimensions d_c and d_f . To the carrier gases: $\sum V_{carrier}$ are collected in the same way as $\sum V_{analytes}$, so do molecular weights. Their viscosities are of the form $C_1 + C_2T$, and the constants are obtained from the analysis by Ettre (33). Further addition of an analyte or column needs only specify these parameters in the JSON file, but its order should be second to last.

Users navigate through the library of ~90 analytes using a search function that matches text input to analyte name. In the current iteration, misspellings and alternate names are intolerable, which may be problematic since chemical nomenclatures vary greatly, and so IUPAC had been used in the entirety of the library to mitigate this issue. Selection of columns and carrier gases are similar, except radio buttons are instead used since their libraries are far smaller. Default values have been set for T , P_0 , and l , but they can vary by user input. P_l is instead set invariably to 1 atm.

The chromatogram is drawn on a canvas element via a `lineTo` function that maps output values (detector response.) and input values (time) to their respective pixels. Some computed parameters are printed on a report table in the bottom part of the screen, and some on an inlay that can be moved but on default set to follow t_R .

The algorithm used in drawing the chromatogram is described in **Fig. 2**. To note: in a temperature programmed elution, T_R is approximated by numerical integration using Simpson's rule with resolution 0.01 °C:

$$\int_{T_0}^{T_R} \frac{dT}{t_M(T) \left[1 + \frac{\alpha}{\beta} e^{\frac{\Delta H}{RT}} \right]} = \int_{T_0}^{T_R} Y(T) dT = r \approx \frac{\Delta T}{3} [Y(T_0) + 4Y(T_1) + 2Y(T_2) + 4Y(T_3) + Y(T_4) + Y(T_5)]$$

With $\Delta T = \frac{T_R - T_0}{4}$. α , β , and ΔH are approximated from a two-point regression of Eq. 11.5 of points T_0 and $T_0 + 10$ K. Widths are approximated by finding k such that t_R in the temperature-programmed elution would equal the isothermal, and H with $T = T_R$ in Eq. 22.

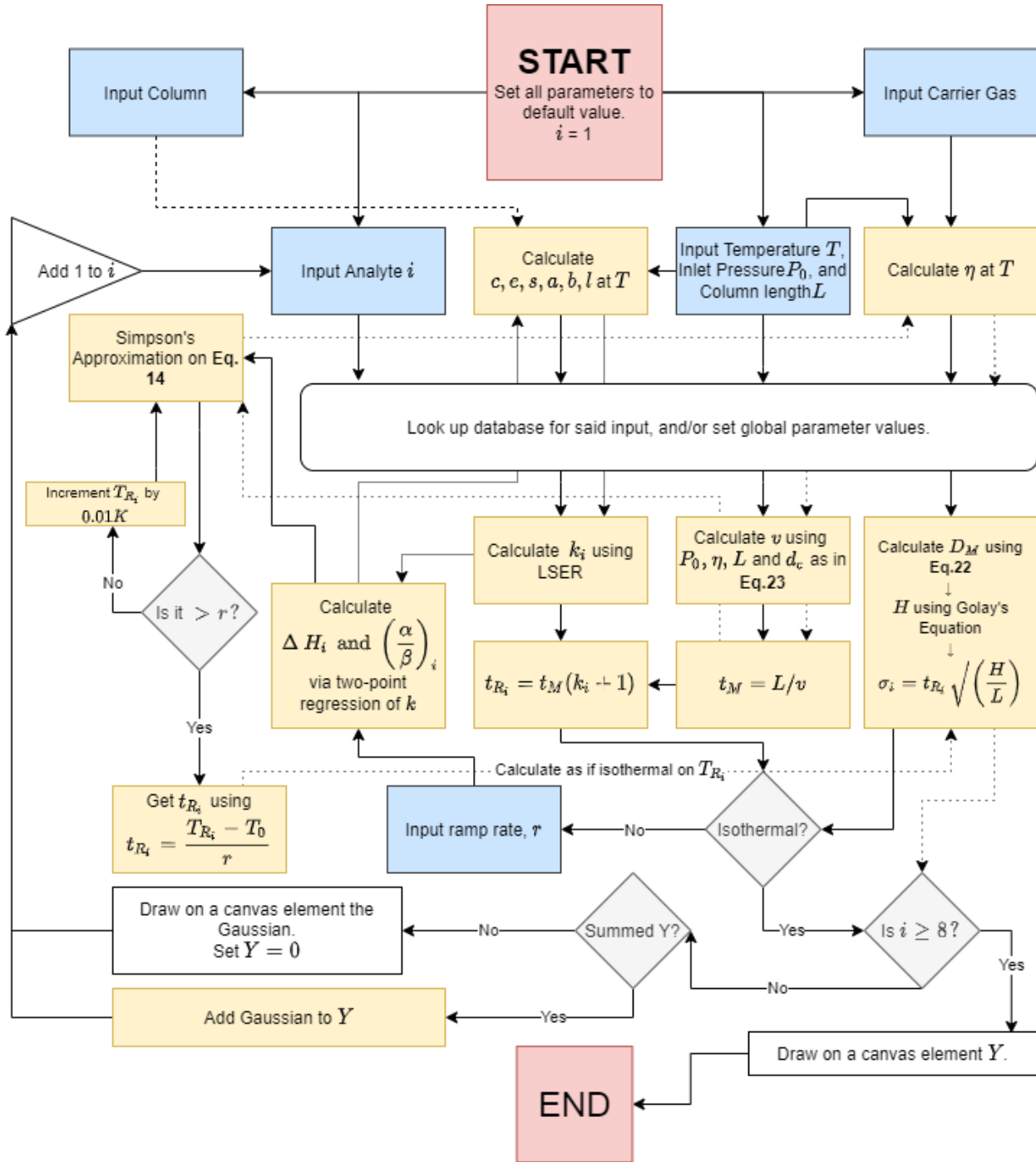


Fig. 2. Flowchart describing the algorithm that draws the chromatogram.

Discussion.

Efforts to review the accuracy of values generated by the simulation tool have largely been drawn from data available in the literature. While it would have been better to independently obtain experimental data, this was not possible because of restrictions due to the novel coronavirus.

Table 1 shows retention times as generated by the simulation tool compared to those obtained by Stone (6) for his 2007 paper pooled from an undergraduate analytical chemistry course. Variable parameters in the simulation tool are set to exactly correspond to experimental settings the data was based upon. Percent deviations are about 10 to 20%, seen increasing as retention time increases, which is markedly higher than those reported by similar studies: Curvers and Rijks (30) had 1-2%, as Snow did (29), while Snyder (31) had 4-6%. To this, temporal wear on the columns used for the elution must be considered, especially since usage in undergraduate courses has diminutive benefit in constant renewal of the columns. Shortening of the column and depletion of the stationary phase components both lead to lessened analyte-column interactions and thus the calculated retention times overshooting the experimental is a direct consequence.

Percent deviation increasing with increasing retention time will in fact be seen in the general case for chromatographic data that follow. One theoretical compromise that might be the cause is the treatment that analyte LSER descriptors E , S , A , B , and L_{16} are constant across all temperatures, which was taken due to the limitation on available data. The other is simply the exponentiation of error since the exponent to $\log(k)$ as modelled with LSER was taken to model t_R . It is also possible that errors arising from instrumental defects compounded. For example, if inlet pressure is different than recorded, then the error is not linear with t_R (so percent deviation is higher for higher t_R), as shown in *Eq. 23* and *Eq. 3*. If temperature control is in defect, then the it compounds further as *Eq. 4* is also considered.

Table 1. Isothermal Retention Times at 90°C of mixture by Stone*

GC-MS, 30m×0.25mm×0.25µm ZB-5, H₂ carrier. $t_M = 1$ min. (6) (Exp.)

30m×0.25mm×0.25µm PTE-5, H₂ carrier. P_0 set such that $t_M = 1$ min. T = 90°C. (Calc.)

Compound	Experimental	Calculated	Percent Deviation
Bromobenzene	2.26	2.5	10.62
Decane	2.82	3.29	16.67
Undecane	4.64	5.53	19.18
Dodecane	8.25	10.18	23.39
Tridecane	15.46	18.88	22.12
Average			18.40

*Retention times in minutes.

Table 2 and 3 show isothermal retention times with the settings on Table 1, but at temperatures 100°C and 115°C respectively. It should be noted that the decrease in percent deviation came as a surprise. Data by Curvers and Rijks (30), Snow (29), and Snyder (31) suggested otherwise, and reasonably so. The computational simplification in which this model is based upon, that is the linearity of column LSER descriptors e, s, a, b , and l to temperature, is equivalent to theirs of $\log(k)$ to temperature. Indeed, as one can plot from **Fig. 1**, the relationship

is nearly linear at lower temperatures but exponential in higher temperatures. The treatment will then underestimate the descriptors leading to the unreliability of the model at extreme temperatures. The trend is indeed seen in Table 4 and 5, suggesting to the singularity in Stone's data that may be caused by column wear.

Table 2. Isothermal Retention Times at 100°C of mixture by Stone*

GC-MS, 30m×0.25mm×0.25µm ZB-5, H₂ carrier. $t_M = 1$ min. (6) (Exp.)

30m×0.25mm×0.25µm PTE-5, H₂ carrier. P_0 set such that $t_M = 1$ min. T = 100°C. (Calc.)

Compound	Experimental	Calculated	Percent Deviation
Bromobenzene	1.91	2.08	8.90
Decane	2.24	2.59	15.63
Undecane	3.39	4.03	18.88
Dodecane	5.59	6.94	24.15
Tridecane	9.81	12.19	24.26
Average			18.36

*Retention times in minutes.

Table 3. Isothermal Retention Times at 115°C of mixture by Stone*

GC-MS, 30m×0.25mm×0.25µm ZB-5, H₂ carrier. $t_M = 1$ min. (6) (Exp.)

30m×0.25mm×0.25µm PTE-5, H₂ carrier. P_0 set such that $t_M = 1$ min. T = 115°C. (Calc.)

Compound	Experimental	Calculated	Percent Deviation
Bromobenzene	1.58	1.67	5.70
Decane	1.74	1.91	9.77
Undecane	2.35	2.66	13.19
Dodecane	3.45	4.06	17.68
Tridecane	5.46	6.54	19.78
Average			13.22

*Retention times in minutes.

Table 4. Isothermal Retention Times at 80°C of Hydrocarbon Sample*

HP-5890 GC, 30m×0.25mm×0.25µm DB-1, H₂ carrier. $t_M = 1.621$ min. T = 80°C. (29) (Exp.)

30m×0.25mm×0.25µm SolGel-1, H₂ carrier. P_0 set such that $t_M = 1.621$ min. T = 80°C. (Calc.)

Compound	Experimental	Calculated	Percent Deviation
Benzene	2.23	2.07	-7.17
Toluene	2.75	2.86	4.00
Octane	3.08	3.28	6.49
Nonane	4.48	4.95	10.49
Decane	7.36	7.95	8.02
Undecane	13.22	14.68	11.04
Dodecane	25.12	29.32	16.72
Tridecane	49.35	57.86	17.24

*Retention times in minutes.

Table 5. Isothermal Retention Times at 100°C of Hydrocarbon Sample*HP-5890 GC, 30m×0.25mm×0.25μm DB-1, H₂ carrier. $t_M = 1.755$ min. T = 100°C. (29) (Exp.)30m×0.25mm×0.25μm SolGel-1, H₂ carrier. P₀ set such that $t_M = 1.755$ min. T = 100°C. (Calc.)

Compound	Experimental	Calculated	Percent Deviation
Benzene	2.122	2.05	-3.39
Toluene	2.41	2.5	3.73
Octane	2.558	2.7	5.55
Nonane	3.228	3.55	9.98
Decane	4.497	4.97	10.52
Undecane	6.897	8.02	16.28
Dodecane	11.413	14.27	25.03
Tridecane	19.895	25.76	29.48

*Retention times in minutes.

Table 6, 7 and 8 show the temperature-programmed retention times as predicted by the simulator compared to experimental data by Snow (29), with starting temperature 60°C single ramped 2°C/min, 8°C/min, and 20°C/min respectively. Percent deviations are lower in about ±1 – 10%, yet are still less accurate than those reported by Snow (1 – 2%), Curvers and Rijks (31) (1 – 2%), and Colmsjo (28) (0.1 – 0.2%). Since physicochemical parameters are derived from the isothermal case, it should be noted that errors will propagate from it. Simulated retention times are closer to the experimental as ramping rate is increased—a trend that is again unexpected. As faster rates result in higher retention temperatures T_R , it should follow promptly that errors arising from the non-linearity of $\log(k)$ to temperature as discussed previously are further compounded. To this it should be noted that incompleteness of the experimental data might be the issue: $t_M = 1.621$ min had been assumed, as it corresponds with the isothermal run, although explicit documentation had not been made in the source data. Regardless, the relevant data at least as we understand it from the literature is only from Snow, since TPGC elution seldom run in single ramp with no hold up time. Future iteration of this simulator will adopt the more complex approach by Snow (28) to facilitate multiple ramps in hope to mitigate this issue. The final trend to be noticed is higher percent deviations for benzene in all three elution, which is likely to be associated with the equilibrium that is yet to be reached as elution proceeds extremely fast.

Table 6. Temperature-programmed Retention Times of Hydrocarbon Sample*

HP-5890 GC, 30m×0.25mm×0.25μm DB-1, H₂ carrier. $t_M = 1.621$ min. $T_0 = 60^\circ\text{C}$. $r = 2^\circ\text{C}/\text{min}$. (29) (Exp.)
30m×0.25mm×0.25μm SolGel-1, H₂ carrier. P_0 set such that $t_M = 1.621$ min. $T = 60^\circ\text{C}$. $r = 2^\circ\text{C}/\text{min}$. (Calc.)

Compound	Experimental	Calculated	Percent Deviation
Benzene	2.45	2.25	-8.16
Toluene	3.35	3.5	4.48
Octane	4.02	4.21	4.73
Nonane	6.35	6.64	4.57
Decane	10.18	10.27	0.88
Undecane	15.42	15.97	3.57
Dodecane	21.57	23.32	8.11
Tridecane	28.04	30.98	10.49

*Retention times in minutes.

Table 7. Temperature-programmed Retention Times of Hydrocarbon Sample*

HP-5890 GC, 30m×0.25mm×0.25μm DB-1, H₂ carrier. $t_M = 1.621$ min. $T_0 = 60^\circ\text{C}$. $r = 8^\circ\text{C}/\text{min}$. (29) (Exp.)
30m×0.25mm×0.25μm SolGel-1, H₂ carrier. P_0 set such that $t_M = 1.621$ min. $T = 60^\circ\text{C}$. $r = 8^\circ\text{C}/\text{min}$. (Calc.)

Compound	Experimental	Calculated	Percent Deviation
Benzene	2.37	2.15	-9.28
Toluene	3.04	3.07	0.99
Octane	3.44	3.51	2.03
Nonane	4.73	4.85	2.54
Decane	6.35	6.45	1.57
Undecane	8.18	8.54	4.40
Dodecane	10.06	10.84	7.75
Tridecane	11.89	13.05	9.76

*Retention times in minutes.

Table 8. Temperature-programmed Retention Times of Hydrocarbon Sample*

HP-5890 GC, 30m×0.25mm×0.25μm DB-1, H₂ carrier. $t_M = 1.621$ min. $T_0 = 60^\circ\text{C}$. $r = 20^\circ\text{C}/\text{min}$. (29) (Exp.)
 30m×0.25mm×0.25μm SolGel-1, H₂ carrier. P_0 set such that $t_M = 1.621$ min. $T = 60^\circ\text{C}$. $r = 20^\circ\text{C}/\text{min}$. (Calc.)

Compound	Experimental	Calculated	Percent Deviation
Benzene	2.28	2.02	-11.40
Toluene	2.73	2.62	-4.03
Octane	2.95	2.87	-2.71
Nonane	3.65	3.59	-1.64
Decane	4.45	4.36	-2.02
Undecane	5.29	5.3	0.19
Dodecane	6.11	6.3	3.11
Tridecane	6.9	7.23	4.78

*Retention times in minutes.

Table 9 shows the retention times and peak widths of the temperature-programmed data by Colmsjo (28) who used the finite element method for prediction, compared to the values as predicted by the simulator. Dodecane, Methyl Decanoate, and 2,6-Dimethylphenol are chosen as analytes, and DB-1, DB-5, DB-17, and DB-23 as columns, since they span the polarity spectrum and thus the predicted values should come as representatives of simulations that follow. Referred data was obtained with 3 minutes hold-up time at 40°C followed by a 4°C/min or 8°C/min single ramp until 120°C. The simulated elution adopts all experimental settings but those, as it is not currently possible to set up multiple ramps, so instead constant ramp starting at $t = 0$ was applied. Regardless, as most analytes neither elute too quickly nor were they too strongly retained, the compromise is reasonable for comparative purposes as shown in the table.

The average absolute percent deviation for retention time and peak width at half height (FWHM) predictions are 9.63% and 39.5%, respectively. The former has been discussed at length, while for the latter better accuracy was observed by Colmsjo of about 15%, which is attributed to the increased computational load as demanded by their method. Peak width being more difficult to predict is in good agreement with data available in the literature, including Colmsjo's which documented lower percent deviation of 0.1 – 0.2% for retention time. One could very well notice that peak widths are more greatly affected by experimental conditions such as injection volume, temperature, and column wear. Even better accuracy was documented in the study by Lamsugarit (32) (5 – 6%), although the performance of its proposed method was evidenced only for alkanes, alcohol, and fatty acid methyl esters in non-polar columns.

Table 9. Calculated and experimental retention times and peak widths of temperature programmed elution.

HP-5890 SERIES GC, 30m×0.25mm×0.25μm for DB-1, DB-5, DB-17, and DB-23. H₂ carrier. $T_0 = 40^\circ\text{C}$.
 Measured gauge pressures are respectively 117.3, 122.3, 124.3 and 117.4 kPa for the 4°C/min, and 117.3, 122.7, 124.0, and 118.0 kPa for the 8°C/min. (28) (Exp.)
 30m×0.25mm×0.25μm for DB-1, PTE-5, DB-17, and DB-23. Other settings identical. (Calc.)

Compound	Retention time (in minutes)	Peak width at half height (in seconds)
----------	-----------------------------	--

Column and Grad.		Exp.	Calc.	Percent Deviation	Exp.	Calc.	Percent Deviation
<i>DB-1</i> 4°C/min	Dodecane	16.47	19.9	20.83	2.82	3.71	31.56
	Methyl Decanoate	20.25	24.4	20.49	2.82	5.54	96.45
	2,6-Dimethylphenol	11.85	14.9	25.74	2.43	1.94	-20.16
8°C/min	Dodecane	11.72	12.89	9.98	1.68	1.63	-2.98
	Methyl Decanoate	13.74	15.28	11.21	2.01	2.26	12.44
	2,6-Dimethylphenol	9.22	9.74	5.64	1.59	1.01	-36.48
<i>DB-5</i> 4°C/min	Dodecane	16.28	18.08	11.06	3	3.39	13.00
	Methyl Decanoate	20.65	23.02	11.48	2.91	5.46	87.63
	2,6-Dimethylphenol	12.54	13.33	6.30	2.61	1.9	-27.20
8°C/min	Dodecane	11.6	11.85	2.16	1.51	1.74	15.23
	Methyl Decanoate	13.97	14.48	3.65	2.23	2.01	-9.87
	2,6-Dimethylphenol	9.61	9.31	-3.12	0.99	1.65	66.67
<i>DB-17</i> 4°C/min	Dodecane	14.38	12.06	-16.13	1.59	3.06	92.45
	Methyl Decanoate	20.84	21.56	3.45	4.97	3.03	-39.03
	2,6-Dimethylphenol	16.83	15.92	-5.41	2.76	2.61	-5.43
8°C/min	Dodecane	10.55	8.48	-19.62	1.71	0.82	-52.05
	Methyl Decanoate	14.07	13.61	-3.27	2.07	2.03	-1.93
	2,6-Dimethylphenol	11.87	10.73	-9.60	1.53	1.32	-13.73
<i>DB-23</i> 4°C/min	Dodecane	5.68	5.8	2.11	4.2	0.38	-90.95
	Methyl Decanoate	16.57	18.13	9.41	3	3.14	4.67
	2,6-Dimethylphenol	21.06	23.82	13.11	2.67	5.4	102.25
8°C/min	Dodecane	5.26	4.63	-11.98	3.09	0.28	-90.94
	Methyl Decanoate	11.62	11.72	0.86	1.74	1.39	-20.11
	2,6-Dimethylphenol	14.21	14.86	4.57	1.95	2.24	14.87
Abs. Average				9.63			39.50

The simulator will be available for open access, and therefore there is merit in kickstarting potential applications. To this, the **supplemental material** as bundled with this paper should be consulted.

One of the exercises that has been included discusses the prevalent misconception, or at least a likely one, that retention can exhaustively be described with boiling point as the variable. Indeed, such is what the student will infer if the eluted mixture consists of all linear alkanes. However, the devil is in the details here as that would assume intermolecular interactions are governed only by London dispersion forces. The exercise then invites the student to think on this concept and would later be shown that a compound with high boiling point (linear alkane >C-30), still elutes faster than a compound with lower (e.g. water) but is more polar, on a polar stationary phase. Similarly, misconceptions like retention time is a function exclusively of carbon number, and temperature affects retention time uniformly on all analytes, are discussed.

Another pedagogical application that has been proposed is the demonstration of industrial and clinical concepts via simulation of lengthy experiments that have previously been impracticable. Kovats retention indices and their experimental determination has been introduced, so did determination of important physical parameters such as molar enthalpy of solution (ΔH) and molar entropy of solution (ΔS) via **Eq.11.5**. The empirical characterisation of **Eq. 19** as done by van Deemter and co-workers has also been suggested in addition to the experimental optimization of resolution via determination of H_{min} . Finally, the capacity of temperature-programmed gas chromatography has been compared to isothermal use in a simulated experimental setting.

The simulator was never intended to replace completely hands-on laboratories, as doing so will bring detriment most to the students. Rather, our hope is that this tool may benefit them by opening the possibility of not only doing more (with less bore), but also to explore experiments that were never introduced in an experiential setting previously due to practical restrictions.

Future Work.

It is regrettable that independently obtained data are minimal in this work. Such data would have been beneficial to review the performance of the simulator more robustly. Similarly, pedagogical applications as one of our primary interest could be enhanced by reviewing student engagement via surveys and evaluations.

There are also features in the simulator that could not be included in the available time. Theoretical foundations of multiple ramp elution in temperature-programmed GC have been established in the paper by Snow. Modelling of peaks using an exponentially modified Gaussian, such that column overloads can be simulated, can also be implemented straightforwardly. Expansion of analyte and stationary phase libraries is another example. Auxiliary features, such as the option to change detectors, automatic optimization of experimental settings, and simulation of noise, had also been in order.

There is plenty of room for improvement on the theoretical side also: in the present iteration it is not possible to have d_c and d_f as variables once a stationary phase has been chosen. This is a result from a discretion on the study upon which stationary phase descriptors are sourced from: c

was defined in terms of k instead of K . To our notice, the best alternatives assume descriptors are constant with temperature and thus are even more irrelevant as then k no longer varies with temperature. Empirical determination of our own is possible, although for that an immense amount of resources and time are to be allocated. In that case, determination of analyte descriptors as functions of temperature, as opposed to otherwise in the current iteration, should also be deemed worthwhile. It is believed that then, levels of accuracy closing into those reported by Curvers and Rijks (1 – 2%), can be achieved.

Finally, polishing of the visual interface of the simulator, porting it to different browsers and devices, and optimization of the codes are to be expected on a future work. Some progress will be made on the remainder of the project tenure.

Conclusion.

It was shown that the predictions made by the gas chromatography simulator as described in this work are in good agreement with experimental data, both for isothermal and temperature-programmed elution. Potential for improvements was noted: multiple ramp TPGC elution modelling will be most critical. Virtual exercises as supplements were designed, although implementation and student evaluation are subject to follow in a future work. Finally, it was argued that virtual laboratories as facilitated by this tool should not completely substitute hands-on laboratories, although at the current iteration the tool should remedy current challenges in chromatographic teaching especially auxiliary consumption of course time and resources.

References.

1. Gerber, F.; Krummen, M.; Potgeter, H.; Roth, A.; Siffrin, C.; Spoendlin, C. Practical Aspects of Fast Reversed-Phase High-Performance Liquid Chromatography Using 3 μ m Particle Packed Columns and Monolithic Columns in Pharmaceutical Development and Production Working under Current Good Manufacturing Practice. *Journal of Chromatography A* **2004**, *1036* (2), 127–133.
2. Datta, A.; Chattaraj, S.; Lahiri, S. Forensic Investigation on the Preparation of Dreaded Alcoholic Beverages without Alcohol Using Gas Chromatography- Fourier Transform Infrared Spectroscopy, Gas Chromatography - Head Space and High Performance Thin Layer Chromatography. *European Journal of Forensic Sciences* **2016**, *3* (4), 1.
3. Esteki, M.; Simal-Gandara, J.; Shahsavari, Z.; Zandbaaf, S.; Dashtaki, E.; Heyden, Y. V. A Review on the Application of Chromatographic Methods, Coupled to Chemometrics, for Food Authentication. *Food Control* **2018**, *93*, 165–182.
4. Skoog, D. A. *Fundamentals of analytical chemistry*; Brooks /Cole, Cengage Learning: Australia, 2014.
5. Sparkman, O. D.; Penton, Z. E.; Kitson, F. G. *Gas chromatography and mass spectrometry: a practical guide*; Elsevier: Amsterdam, 2011.
6. Stone, D. C. Teaching Chromatography Using Virtual Laboratory Exercises. *Journal of Chemical Education* **2007**, *84* (9), 1488.
7. Reijenga, J. GCSIM: A Gas-Liquid Chromatography Simulator for Educational Purposes. *Journal of Chromatography A* **1991**, *588* (1-2), 217–224.

8. Yuan, M. Gas Chromatographic Simulation Program. *Journal of Chemical Education* **1977**, *54* (6), 364.
9. COMSOL Multiphysics® v. 5.4. www.comsol.com. (accessed Aug 18, 2020).
10. DryLab. <http://molnar-institute.com/drylab> (accessed Aug 18, 2020).
11. Abraham, M. H.; Ibrahim, A.; Zissimos, A. M. Determination of Sets of Solute Descriptors from Chromatographic Measurements. *Journal of Chromatography A* **2004**, *1037* (1-2), 29–47.
12. Vitha, M.; Carr, P. W. The Chemical Interpretation and Practice of Linear Solvation Energy Relationships in Chromatography. *Journal of Chromatography A* **2006**, *1126* (1-2), 143–194.
13. Curvers, J.; Rijks, J.; Cramers, C.; Knauss, K.; Larson, P. Temperature Programmed Retention Indices: Calculation from Isothermal Data. Part 1: Theory. *Journal of High Resolution Chromatography* **1985**, *8* (9), 607–610.
14. Grant, D.; Hollis, M. Practical Approach to the Theory of Linear Programmed Temperature Gas Chromatography with Particular References to the Analysis of Aromatic Hydrocarbons. *Journal of Chromatography A* **1978**, *158*, 3–19.
15. Giddings, J. C. *Dynamics of chromatography*; M. Dekker: New York, 1965.
16. J. N. Wilson. A Theory of Chromatography. *Journal of the American Chemical Society* **1940**, *62* (6), 1583-1591.
17. Martin, A. J. P.; Synge, R. L. M. A New Form of Chromatogram Employing Two Liquid Phases. *Biochemical Journal* **1941**, *35* (12), 1358–1368.
18. Deemter, J. V.; Zuiderweg, F.; Klinkenberg, A. Longitudinal Diffusion and Resistance to Mass Transfer as Causes of Nonideality in Chromatography. *Chemical Engineering Science* **1995**, *50* (24), 3869–3882.
19. M.J.E. Golay, Theory of chromatography in open and coated tubular columns with round and rectangular cross-sections, in: D.H. Desty (Ed.), *Gas Chromatography 1958* (Amsterdam Symposium), Butterworths, London, 1958, pp. 36–55
20. Fuller, E. N.; Schettler, P. D.; Giddings, J. C. New Method For Prediction Of Binary Gas-Phase Diffusion Coefficients. *Industrial & Engineering Chemistry* **1966**, *58* (5), 18–27.
21. Fuller, E. N.; Ensley, K.; Giddings, J. C. Diffusion of Halogenated Hydrocarbons in Helium. The Effect of Structure on Collision Cross Sections. *The Journal of Physical Chemistry* **1969**, *73* (11), 3679–3685.
22. Karaiskakis, G.; Gavril, D. Determination of Diffusion Coefficients by Gas Chromatography. *Journal of Chromatography A* **2004**, *1037* (1-2), 147–189.
23. Arnold, H. Studies in Diffusion. *Industrial and Engineering Chemistry* **1930**, *20* (10), 1091–1095.
24. Gilliland, E. R. Diffusion Coefficients in Gaseous Systems. *Industrial & Engineering Chemistry* **1934**, *26* (6), 681–685.
25. Hirschfelder, J. O.; Curtiss, C. F.; Bird, R. B. *Molecular theory of gases and liquids*; Wiley: Hoboken, NJ, 2010.
26. Michell, S. J. (S. J. *Fluid and particle mechanics*; Pergamon: Oxford, 1970.
27. Cramers, C. A.; Rijks, J. A.; Schutjes, C. P. M. Factors Determining Flow Rate in Chromatographic Columns. *Chromatographia* **1981**, *14* (7), 439–444.
28. Aldaeus, F.; Thewalim, Y.; Colmsjö, A. Prediction of Retention Times and Peak Widths in Temperature-Programmed Gas Chromatography Using the Finite Element Method. *Journal of Chromatography A* **2009**, *1216* (1), 134–139.

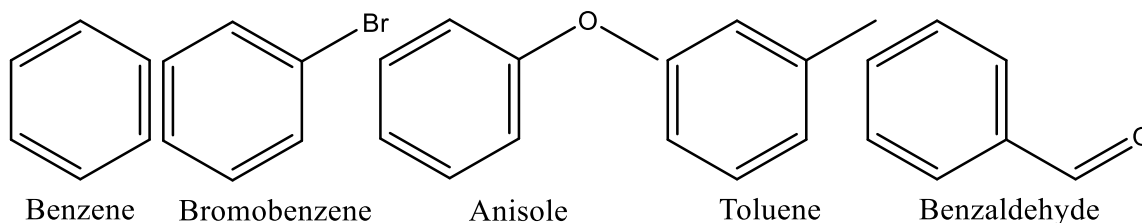
29. Snow, N. H.; Mcnair, H. M. A Numerical Simulation of Temperature-Programmed Gas Chromatography. *Journal of Chromatographic Science* **1992**, *30* (7), 271–275.
30. Curvers, J.; Rijks, J.; Cramers, C.; Knauss, K.; Larson, P. Temperature Programmed Retention Indices: Calculation from Isothermal Data. Part 2: Results with Nonpolar Columns. *Journal of High Resolution Chromatography* **1985**, *8* (9), 611–617.
31. Bautz, D. E.; Dolan, J. W.; Raddatz, W. D.; Snyder, L. R. Computer Simulation (Based on a Linear-Elution-Strength Approximation) as an Aid for Optimizing Separations by Programmed-Temperature Gas Chromatography. *Analytical Chemistry* **1990**, *62* (15), 1560–1567.
32. Lomsugarit, S.; Krisnangkura, K. An Alternative Approach for Predicting Peak Width in Gas Chromatography. *Chromatographia* **2002**, *56* (1-2), 99–103.
33. Ettre, L. S. Viscosity of Gases Used as the Mobile Phase in Gas Chromatography. *Chromatographia* **1984**, *18* (7), 413–413.
34. Poole, C. F. Gas Chromatography System Constant Database for 52 Wall-Coated, Open-Tubular Columns Covering the Temperature Range 60–140 °C. *Journal of Chromatography A* **2019**, *1604*, 460482.
35. Poole, C. F.; Atapattu, S. N.; Poole, S. K.; Bell, A. K. Determination of Solute Descriptors by Chromatographic Methods. *Analytica Chimica Acta* **2009**, *652* (1-2), 32–53.
36. Siriviboon, P.; Tungkaburee, C.; Weerawongphrom, N.; Kulsing, C. Direct Equations to Retention Time Calculation and Fast Simulation Approach for Simultaneous Material Selection and Experimental Design in Comprehensive Two Dimensional Gas Chromatography. *Journal of Chromatography A* **2019**, *1602*, 425–431.
37. National Institute of Health. <https://www.nih.gov/> (accessed Aug 19, 2020).
38. Boswell, P. GC Simulator. <http://www.gcsimulator.org/about/index.php> (accessed Aug 19, 2020).
39. ProEZGC. <https://www.restek.com/proezgc> (accessed Aug 19, 2020).

Supplementary exercises.

Q1. Boiling point and Polarity.

Retention in gas chromatography is dependent on the strength of intermolecular forces both within the analyte itself and between the analyte and the stationary phase it is run on.

- a. As a refresher, look up the normal boiling points and sort the following compounds in order of increasing polarity:



- b. Use the GC Simulator to run this set of compounds on a polar stationary phase. Choose a column temperature that ensures all peaks are separated at the baseline. How does adjusted retention time vary with boiling point for this set of compounds?
- c. Use Excel to plot the data and find a relationship between these parameters.
- d. You have been given an unknown homogenous liquid that boils at 170 °C (1 atm). Using your results from parts **b and c**, predict where this compound will elute relative to the other compounds .

[345Hcv sua] Let us now consider a set of compounds whose polarities are approximately equal.

- e. Plot $\log(t_R')$ as a function of #carbon and $\log(t_R')$ as a function of boiling point. Report your R^2 and notice that both bear high degrees of linearity. This is a curious case. Explain how this came about. (Hint: consider ΔH°)

Your result in *d* is in fact the foundation of the normalized indexing system Kovats retention index, *I*:

$$I = 100 \left(n + \frac{\log(t_{R_i}) - \log(t_{R_n})}{\log(t_{R_{n+1}}) - \log(t_{R_n})} \right)$$

Where *n* is the #carbon of a straight alkane with retention time t_{R_n} .

- f. Why is indexing t_{R_i} directly not preferable for analyte *i*?
- g. Index the analyte **anisole at multiple flow rates, temperature, and column length**. Confirm with an [online database](#). Report your calculations.

Q2. Temperature.

Equilibrium is never fully achieved at any point in the column. However, if one considers the entirety of the stationary phase in competition with the entirety of the mobile phase over the analyte, then indeed the partition coefficient *K* is a useful measure as thermodynamic laws describing systems in equilibrium do apply.

- a. Explain why the first sentence of the preamble is true. Alternatively, why the converse cannot be true.

Consider the van 't Hoff equation:

$$\ln(K) = -\frac{\Delta H^\circ}{R} \left(\frac{1}{T} \right) + \frac{\Delta S^\circ}{R}$$

- b. [piHcvhua]. You wish to determine the standard change of partition enthalpy (ΔH°) and the standard change of partition entropy (ΔS°) of **one** analyte in your system. Assuming both values are independent of *T*, how would you go about accomplishing this? Report your quantitation.
- c. Determine $\frac{dK}{dT}$, under the same assumptions as in **b**. Is the value of this term zero, negative, or positive? Explain why.

- d. Increase the temperature of your run up until 300 °C. Report anything you find unusual and explain why.

Q3. Plate Height and Peak Width.

The plate theory of chromatography bears some unreasonable assumptions.

- a. Elaborate on **one** of those assumptions.

It is said that the theory is then useful only for conceptual purposes. Regardless, there are numerous works in GC that are based on the plate theory. Since most only uses the relation

$FWHM = t_R \sqrt{\frac{5.54}{H}} L$, plate theory is considered useful for descriptive purposes. Consider the van Deemter equation:

$$H = A + \frac{B}{u} + Cu$$

- b. As a refresher, describe A, B, and C concisely.

In capillary gas chromatography however, that equation often carries redundancy. Golay's equation is then more frequently used:

$$H = \frac{B}{u} + (C_s + C_m)u$$

- c. Why is it that the A term in the van Deemter equation is considered negligible?

It is desirable that H is minimal, as then peak widths are narrow and hence discernible.

- d. Determine, as function of B, C_s , and C_m , the linear flow velocity u , where H is minimal (H_{min}).
- e. u is not a variable in the GC Simulator. However, u can be derived easily from flow rate and column dimensions. Express u as a function of flow rate v , internal diameter d_c , and film thickness d_f .
- f. Propose an experiment where you can reasonably estimate H_{min} . Run that experiment on the operating conditions of your choice. Report H_{min} .

Q4. Temperature Gradient.

to follow. check the link to the simulator for possible updates.